UDC 629.064.5 https://doi.org/10.33619/2414-2948/81/28

DYNAMIC PRICING AND ENERGY MANAGEMENT OF ELECTRIC HEATING INTEGRATED ENERGY SYSTEM BASED ON STACKELBERG GAME

©**Wang Yibo,** *Jiangsu University of Science and Technology, Zhenjiang, China; Mordovia State University, Saransk, Russia; 209210040@stu.just.edu.com*
©**Feng Guozeng,** *Jiangsu University of Science and Technology, Zhenjiang, China; Mordovia State University, Saransk, Russia*

ДИНАМИЧЕСКОЕ ЦЕНООБРАЗОВАНИЕ И УПРАВЛЕНИЕ ЭНЕРГИЕЙ ИНТЕГРИРОВАННОЙ ЭНЕРГЕТИЧЕСКОЙ СИСТЕМЫ ЭЛЕКТРООБОГРЕВА НА ОСНОВЕ ИГРЫ ШТАКЕЛЬБЕРГА

©**Ван Ибо,** *Цзянсуский университет науки и технологий, г. Чжэньцзян, Китай; Национальный исследовательский Мордовский государственный университет им. Н.П. Огарева, г. Саранск, Россия; 209210040@stu.just.edu.com*
©**Фэн Гоцзэн,** *Цзянсуский университет науки и технологий, г. Чжэньцзян, Китай; Национальный исследовательский Мордовский государственный университет им. Н.П. Огарева, г. Саранск, Россия*

Abstract. This paper investigates the dynamic pricing and energy management of integrated electric and thermal energy systems through the Stackelberg game approach, for the upper tier leader problem, the revenue of the integrated energy system as a whole is used as the objective function, taking into account the electricity price and related constraints such as the heat price, for the lower follower problem, a leader-follower Stackelberg game model is constructed with the highest user satisfaction as the objective function, Constraints such as power balance conditions and thermal balance conditions of the system are also taken into account, The upper level of the model is solved using a differential evolutionary algorithm, Lower level solver using CPLEX solver. The simulation results show that the proposed model not only effectively weighs the interests of the integrated energy system and the customer aggregator, but also achieves a win-win situation for both the customer aggregator and the external grid, and the solution algorithm used protects the data privacy between the integrated energy system and the customer aggregator.

Аннотация. В данной работе исследуется динамическое ценообразование и управление энергией в интегрированных электрических и тепловых энергетических системах с помощью подхода игры Штакельберга. Для проблемы лидера верхнего уровня в качестве целевой функции используется доход интегрированной энергетической системы в целом, принимая во внимание цену на электроэнергию и связанные ограничения, такие как цена на тепло. Для проблемы нижнего уровня последователя строится модель игры лидер-последователь Штакельберга с наибольшим удовлетворением пользователя в качестве объективной функции. Учитываются такие ограничения, как условия баланса мощности и условия теплового баланса системы. Верхний уровень модели решается с помощью дифференциального эволюционного алгоритма, нижний уровень решается с помощью решателя CPLEX. Результаты моделирования показывают, что предложенная модель не только эффективно взвешивает интересы интегрированной энергетической системы и агрегатора потребителей, но и достигает беспроигрышной ситуации как для агрегатора потребителей, так и для внешней

Тип лицензии CC: Attribution 4.0 International (CC BY 4.0)

сети, а используемый алгоритм решения защищает конфиденциальность данных между интегрированной энергетической системой и агрегатором потребителей.

Keywords: Stackelberg game, integrated energy systems, dynamic pricing, energy management.

Ключевые слова: игра Штакельберга, интегрированные энергетические системы, динамическое ценообразование, управление энергией.

With the full development of clean energy sources such as wind and photovoltaic power generation and the development and use of technologies such as cogeneration and microgrids, China is pushing forward with its energy transition, while in the international environment, many countries are also deepening their energy structures [92]. However, in recent decades, with rapid economic development, population growth and rising living standards, fossil fuel consumption has increased dramatically, leading to serious energy-related problems, such as energy shortages and environmental pollution, which have become pressing themes in the world's energy sector [93, 94].

We have been making active efforts in the field of energy saving and emission reduction. According to the Global Coal Market Report (2018–2023) published by the International Energy Agency in 2019, China's economy and energy environment are in a period of structural transformation and the share of coal demand is set to decline year on year. In the following five years, the share of coal resources in the global energy mix will be reduced from 27% to 25%, and it will be replaced mainly by clean energy sources such as renewable energy and natural gas. China's total coal resources will increase from 4.1 billion tons in 2020 to over 4.2 billion tons in 2030, and although the total will increase, its share will decrease by 8% [95]. In 2020, the country proposes a dual carbon target of 3060: striving to peak CO2 emissions by 2030 and striving to achieve carbon neutrality by 2060.In order to reduce greenhouse gas emissions and fossil fuel consumption, there are two possible technological routes to this end: one effective way is to increase the ratio of renewable energy to primary energy in the power system, of which the application of wind power and photovoltaic power generation has received the most attention among the many technologies that use renewable energy for clean power generation; the other effective way is to increase the energy efficiency of power plants, one of the most effective ways to achieve this is through combined heat and power technology [96].

Combined Heat and Power (CHP) has gained increasing attention in recent years due to its high efficiency, environmental friendliness, reliability and economic efficiency, which not only effectively addresses the energy shortage crisis, but also significantly reduces the environmental pollution generated during operation [97, 98]. In theory, the efficiency of CHP systems can often be as high as 80% or even higher, and because of this, many countries around the world are actively promoting the application of CHP technology [99]. However, the shortcomings of the combined electric and thermal system are gradually revealed. The heat generating units used in the combined electric and thermal system are mainly combined heat and power units, which contain both heat and power, and there is a strong coupling between heat and power [100].In the northern heating season, for example, the installed capacity of CHP units is relatively high, while the proportion of peaking units is small, and the peaking capacity is poor. This is because there is no direct conversion between electricity and heat, and units tend to operate in a "heat to power" mode, where the operation of CHP units is constrained by the minimum power output in order to maintain the heating level of the system, resulting in the grid receiving less wind power [10].

Тип лицензии CC: Attribution 4.0 International (CC BY 4.0)

Т. 8. №8. 2022
https://doi.org/10.33619/2414-2948/81

In the context of world energy shortage and serious environmental pollution, clean energy has become the mainstream trend in energy development [11]. However, its large-scale entry into the grid poses a huge challenge to the safe operation of the grid. Virtual power plant (VPP) is one of the main solutions to the problem of grid integration of multiple distributed energy resources (DER), effectively aggregating distributed power sources, energy storage and controllable loads to form a virtual whole to participate in the electricity market and the operation and dispatch of the grid [12], which will become an important link in the promotion of smart grid construction.

This paper proposes a game-theoretic algorithm to ensure the deployment of clean energy and other energy sources to the grid in order to meet the requirements of low cost and green energy supply by ensuring the deployment of customer demand and power plant capacity.

The integrated cogeneration energy system studied in this paper consists of two parts, the power supply part and the heat supply part. The power supply part consists of the CHP unit and the scenic storage equipment, while the heat supply part consists of the CHP unit and the gas boiler. The composition of the integrated energy system is shown in Figure 1.

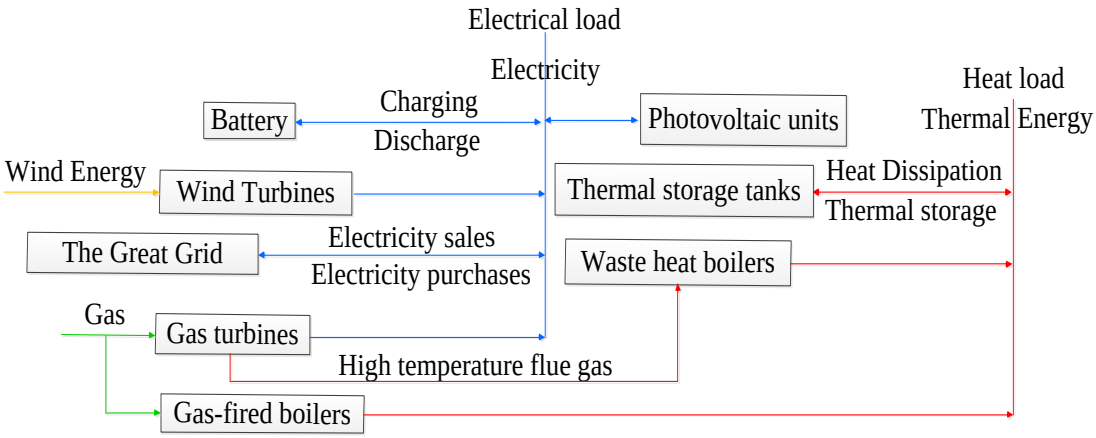

Figure 1. Integrated energy system components

In combined heat and power systems, the output of wind turbines can be constrained by the size and practicality of the installed capacity.When the installed capacity is determined, the maximum value of wind power output at each moment is determined by the actual conditions such as weather and environment, and the wind turbine generation capacity P_{wz} and the wind speed at moment t satisfy the following non-linear relationship [13].

$$\begin{cases} 0 & v(t) < v_i \ or \ v(t) > v_0 \\ \dfrac{P_{WZ}(v(t)-v_i)}{v_r - v_i} & v_i \le v(t) \le v_r \\ P_{WZ} & v_r \le v(t) \le v_0 \end{cases} \quad (1)$$

Where, $v(t)$ is the real-time wind speed at time t, v_i is the cut-in wind speed, v_0 is the cut-out wind speed, v_r is the rated wind speed, P_{wz} is the installed capacity of the wind turbine. When the real-time wind speed is less than the cut-in wind speed or greater than the cut-out wind speed, the WTGs are shut down. When the real-time wind speed is greater than the cut-in wind speed and less than the rated wind speed, the real-time power generation and the wind speed satisfy the primary function,

Тип лицензии CC: Attribution 4.0 International (CC BY 4.0)

Т. 8. №8. 2022
https://doi.org/10.33619/2414-2948/81

when the real-time wind speed is greater than the rated wind speed and less than the cut-out wind speed, the value of the real-time power generation is equal to the value of the installed capacity.

The power generated by photovoltaics is related to light intensity and temperature and is mathematically modelled as follows [14].

$$P_{pvt} = \alpha_{pv} P_{PVZ} \frac{A_t}{A_s}[1 + \alpha_T (T - T_{stp})] \quad (2)$$

Where, α_{pv} is the power derating factor of the unit, P_{PVZ} is the rated power of the PV, A_t is the actual irradiance of the PV at moment t, A_s is the irradiance at standard conditions (in units: kw/m^2). α_T is the power temperature coefficient, and T_{sp} is the temperature at standard conditions. Since the value of α_T is relatively very small, the effect of temperature variation on the output of the PV unit is approximately zero, so the power generated by the PV can be approximately proportional to the actual irradiance.

Electric storage systems store electrical energy, allowing the power to be panned in the time dimension to meet the requirements of the stochastic nature of new energy generation. At present, the electric energy storage technologies used in integrated energy systems include lead-acid, sodium-sulphur, liquid-flow and nickel-chromium batteries. Lead-acid batteries are often chosen as electrical energy storage components due to their small self-discharge rate, high discharge rate, low price and low charging and discharging losses：

To avoid the adverse effects of charging and discharging at low power and low charge states on lifetime, the battery is operated to meet the charging and discharging constraints and the charge state constraints [15], i.e.

$$\begin{aligned} U^t_{bt.chr} P^{\min}_{bt.chr} \le P^t_{bt.chr} \le U^t_{bt.chr} P^{\max}_{bt.chr} \\ U^t_{bt.dis} P^{\min}_{bt.dis} \le P^t_{bt.dis} \le U^t_{bt.dis} P^{\max}_{bt.dis} \end{aligned} \quad (3)$$

$$\begin{aligned} SOC^t_{bt} = SOC^{t-1}_{bt} + (\eta_{bt.chr} P^t_{bt.chr} - P^t_{bt.dis} / \eta_{bt.dis})\Delta t \\ SOC^{\min}_{bt} \le SOC^t_{bt} \le SOC^{\max}_{bt} \end{aligned} \quad (4)$$

Where: SOC^t_{bt} is the state of charge of the battery, kWh; *Pt bt.chr* and *Pt bt.dis* are the charging and discharging power of the battery, kW; $\eta_{bt.chr}$ and $\eta_{bt.dis}$ are the charging and discharging efficiency of the battery; *Ut bt.chr* and *Ut bt.dis* are the charging and discharging state marker bits of the battery, 0 for out of service, 1 for operation; and satisfy Mutual exclusion constraint and charging and discharging frequency constraint, i.e.

$$U^t_{bt.dis} + U^t_{bt.chr} \le 1 \quad (2)$$

$$\sum_{t=1}^{24} U^t_{bt.dis} + U^t_{bt.chr} \le T \quad (3)$$

In actual operation, the battery has to meet the charge/discharge creep rate constraint.

Тип лицензии CC: Attribution 4.0 International (CC BY 4.0)

$$P_{bt.chr}^{down} \le P_{bt.chr}^{t} - P_{bt.chr}^{t-1} \le P_{bt.chr}^{up}$$
$$P_{bt.dis}^{down} \le P_{bt.dis}^{t} - P_{bt.dis}^{t-1} \le P_{bt.dis}^{up} \quad (4)$$

Where: $P_{bt.chr}^{down} / P_{bt.chr}^{up}$ and $P_{bt.dis}^{down} / P_{bt.dis}^{up}$ are the minimum/large charging and discharging power of the battery in charging and discharging state respectively, kW.

Thermal storage tanks can store thermal energy when it is in surplus and release it when it is in short supply or when it is more expensive to produce heat, improving the flexibility and economy of system operation [16].

$$W_{tst}^{t} = W_{tst}^{t-1}(1-\gamma_h) + (\eta_{tst.chr} H_{tst.chr}^{t} - H_{tst.dis}^{t} / \eta_{tst.dis})$$
$$W_{tst}^{\min} \le W_{tst}^{t} \le W_{tst}^{\max} \quad (5)$$

$$U_{tst.chr}^{t} H_{tst.chr}^{\min} \le H_{tst.chr}^{t} \le H_{tst.chr}^{\max} U_{tst.chr}^{t}$$
$$U_{tst.dis}^{t} H_{tst.dis}^{\min} \le H_{tst.dis}^{t} \le H_{tst.dis}^{\max} U_{tst.dis}^{t} \quad (6)$$

where: W_{tst}^{t} is the stored thermal energy of the storage tank, kWh; $H_{tst.chr}^{t}$ and $H_{tst.dis}^{t}$ are the storage and discharge thermal power of the storage tank, respectively, kW; γ_h is the energy self-loss rate of the storage tank; $\eta_{tst.chr}$ and $\eta_{tst.dis}$ are the storage efficiency and discharge efficiency, respectively; *Ut tst.chr* and *Ut tst.dis* are the charging and discharging status marker bits of the storage tank and 0 for stop and 1 for run; and satisfy the mutual exclusion constraint, i.e.:

$$U_{tst.dis}^{t} + U_{tst.chr}^{t} \le 1 \quad (7)$$

Same operating mode as the battery, to meet the climbing rate constraint.

$$H_{tst.chr}^{down} \le H_{tst.chr}^{t} - H_{tst.chr}^{t-1} \le H_{tst.chr}^{up}$$
$$H_{tst.dis}^{down} \le H_{tst.dis}^{t} - H_{tst.dis}^{t-1} \le H_{tst.dis}^{up} \quad (8)$$

Where: *Hdown tst.chr*/*Hup tst.chr* and *Hdown tst.dis*/*Hup tst.dis* are the minimum/large storage and discharge power in the storage and discharge state of the thermal storage tank respectively, kW.

Cogeneration units are generally divided into two types: pumped condensing units and back pressure units. Back pressure units have a high thermal cycle efficiency but poor adaptability to load changes, while pumped condensing units have good electrical and thermal mutual adjustability, but a relatively low heat supply, and most cogeneration units in China currently use pumped condensing units. In this paper, the whole turbine is composed of three parts: low pressure cylinder, medium pressure cylinder and high pressure cylinder.The high temperature and high pressure steam produced in the waste heat boiler enters the turbine to do work, the heat extraction comes from the medium pressure cylinder discharge, and the rest of the steam is put into the low pressure cylinder to do work and then into the condenser condensation, and then back to the boiler to achieve repeated use. Based on the above principle, the gas turbine in the cogeneration system generates electricity while the waste heat produced is outputted through the waste heat boiler, and its electricity and heat output expressions are [17].

Тип лицензии CC: Attribution 4.0 International (CC BY 4.0)

Т. 8. №8. 2022
https://doi.org/10.33619/2414-2948/81

$$\begin{cases} G_{GT}^{t} = a(P_{GT}^{t})^{2} + bP_{GT}^{t}) + cI_{GT}^{t} \\ H_{HE}^{t} = \eta^{\mathrm{GT}} P_{GT}^{t}) / \lambda^{\mathrm{GT}} \end{cases} \quad (9)$$

Where: *Gt GT*、*Pt GT* and *Ht HE* are the natural gas power consumed by the GT, the output electric power and the waste heat power recovered from the power generation through the waste heat boiler respectively; *It GT* is a 0-1 variable indicating the on/off state of the micro gas turbine; *a*, *b* and *c* are the fuel consumption coefficients; λGT is the output electric and thermal power ratio of the micro gas turbine; ηGT is the heat recovery efficiency.

GT operation is also subject to operating power constraints and climbing constraints:

$$\begin{cases} P_{\min}^{\mathrm{GT}} \le P_{GT}^{t} \le P_{\max}^{\mathrm{GT}} \\ P_{\mathrm{down}}^{\mathrm{GT}} \le P_{GT}^{t} - P_{GT}^{t-1} \le P_{\mathrm{up}}^{\mathrm{GT}} \end{cases} \quad (10)$$

Where: *PGT* min、*PGT* max are the upper and lower limits of the output electric power of the gas turbine; *PGT* up、*PGT* down are the upper and lower limits of the climbing power of the gas turbine.

GB generates heat by burning natural gas to supplement the thermal load when the GT does not produce enough heat, and its output thermal power *H*GB *t* is related to the input natural gas power *Gt GB* as [18]:

$$\begin{cases} H_{GB}^{t} = \eta^{\mathrm{GB}} G_{GB}^{t} \\ 0 \le H_{GB}^{t} \le H_{\max}^{\mathrm{GB}} \end{cases} \quad (11)$$

Where: η^{GB} is the heat production efficiency of the GB; *HGB* max is the upper limit of the thermal power output of the GB.

The integrated energy system can buy and sell electricity to the external distribution grid to maintain the balance of the electrical load within the system. To ensure the safe operation of the distribution grid, the integrated energy system cannot purchase and sell electricity to the grid at the same time, and the upper limit of the interactive power with the distribution grid is specified within a certain range to meet the following constraints [19]:

$$I_{t}^{\mathrm{bGrid}} + I_{t}^{\mathrm{sGrid}} \le 1 \quad (12)$$

$$\begin{cases} 0 \le P_{t}^{\mathrm{bGrid}} \le P_{\max}^{\mathrm{bGrid}} \\ 0 \le P_{t}^{\mathrm{sGrid}} \le P_{\max}^{\mathrm{sGrid}} \end{cases} \quad (13)$$

Where: *I*bGrid *t* and *I*sGrid *t* are 0-1 variables indicating the power purchase and sale status of the integrated energy system at time *t*; *P*bGrid *t* and *P*sGrid *t* are the power purchase and sale of EH; *P*bGrid *max* and *P*sGrid *max* are the upper limits of the power purchase and sale of the integrated energy system.

The integrated energy operator can be seen as an energy hub with a two-way energy flow, playing the role of energy production, transmission and supply. It is the leader and coordinator of the

Тип лицензии CC: Attribution 4.0 International (CC BY 4.0)

Т. 8. №8. 2022
https://doi.org/10.33619/2414-2948/81

integrated energy system, taking on the responsibility of balancing the power of the source, load and storage of the main market investors, playing the role of a manager, and the customer can interact with the integrated energy operator through feedback on energy demand. The price strategy is formulated on the basis of the capacity plan of its own supply equipment and the load demand on the energy side, with the optimisation objective of maximising returns, which can be expressed as:

$$\max E_{eso} = \sum_{t=1}^{T} (C_{sell} - C_{grid} - C_{CCHP} - C_h) \tag{14}$$

Where *Ct sell* represents the revenue from supplying energy to the user side at time *t*. *Ct grid* represents the grid interaction cost, when it is greater than 0 it represents the purchase of electricity from the grid, otherwise it represents the sale of electricity to the grid, and C_h represents the cost of operating and maintaining the equipment. *C CCHP* represents its fuel cost. The above equations can be expressed as follows:

$$C_{sell}^t = (P_{el}^t c_{e,s}^t + Q_{hl}^t c_{h,s}^t)\Delta t \tag{15}$$

$$C_{grid}^t = [\max(P_{el}^t - P_{es}^t, 0)c_{g,s}^t + \min(P_{el}^t - P_{es}^t, 0)c_{g,b}^t]\Delta t \tag{16}$$

$$C_h = \sum_i K_i P_i^t \tag{17}$$

$$C_{cchp}^t = a_e (P_{GT}^t)^2 + b_e P_{GT}^t + c_e + a_h (Q_{GB}^t)^2 + b_h Q_{GB}^t + c_h \tag{18}$$

where *Pt el* and *Qt hl* denote the electrical and thermal loads of the customer, respectively, *ct e,s* and *ct h,s* denote the price at which the operator sells electricity and heat to the customer, respectively,*ct g,s* and *ct g,b* denote the price at which the operator sells and purchases electricity from the external grid, respectively, and *Pt es* denotes the total amount of electricity supplied by the operator. K_i denotes the equipment operation and maintenance factor; *Pt GT* and *Qt GB* denote the electric power output of the gas turbine and the thermal power output of the gas boiler. In addition, a_e, b_e, c_e, a_h, b_h and c_h denote the fuel cost factors for gas turbines and gas boilers respectively.

In addition, to prevent the problem from degenerating and to avoid direct transactions between the energy-using side and the grid, it should be ensured that the operator sells at a price slightly below the market price, and the following constraints need to be met:

$$c_{g,b}^t < c_{e,s}^t < c_{g,s}^t \tag{19}$$

$$c_{h,\min}^t < c_{h,s}^t < c_{h,\max}^t \tag{20}$$

Users optimize their own power consumption of electricity and heat loads on the basis of a price given by the energy operator for the sale of energy, with the aim of maximising consumer surplus, i.e., the difference between the user's utility function and the cost of using energy. This can be expressed as

$$F_{user} = \sum_{t=1}^{T} (f_u^t - (P_{el}^t c_{e,s}^t + Q_{hl}^t c_{e,h}^t)\Delta t \tag{21}$$

Тип лицензии CC: Attribution 4.0 International (CC BY 4.0)

Т. 8. №8. 2022
https://doi.org/10.33619/2414-2948/81

where *f* represents the user's utility function, indicating the degree of satisfaction obtained by the user in purchasing electrical and thermal energy, usually non-decreasing and convex, with several forms such as quadratic and logarithmic, etc. This paper uses the quadratic function to represent:

$$f_u^t = v_e P_{el}^t - \frac{\alpha_e}{2}(P_{el}^t)^2 + v_h P_{hl}^t - \frac{\alpha_h}{2}(P_{hl}^t)^2 \quad (22)$$

where: v_e , α_e , v_h and α_h denote preference coefficients for the consumption of electrical and thermal energy respectively, which can reflect the consumer's preference for energy and influence the magnitude of demand.

The consumer electrical load contains both fixed and levelizable electrical loads and can be expressed as:

$$P_{el}^t = P_{fel}^t + P_{sel}^t \quad (23)$$

Among them, *Pt fel* denotes fixed load, which requires high reliability of power supply and is not easy to change, ensuring normal production and life of users; *Pt sel* denotes transferable load, which allows users to reasonably adjust their energy consumption load according to the price of energy sales given by the operator, but needs to meet the following constraints:

$$\begin{aligned} 0 \le P_{sel}^t \le P_{sel}^{\max} \\ \sum_{t=1}^{T} P_{sel}^t \Delta t = W_{sel} \end{aligned} \quad (24)$$

where *Pmax sel* denotes the upper limit of user transferable load and W_{sel} denotes the total amount of transferable load in *T* time periods, i.e., the total amount of transferable load needs to be kept constant before and after the demand response.

In addition, the thermal loads in the text are similar, containing both fixed and transferable loads, as follows:

$$Q_{hl}^t = Q_{fhl}^t + Q_{shl}^t \quad (25)$$

$$0 \le Q_{shl}^t \le Q_{shl}^{\max} \quad (26)$$

Where *Qt fhl* and *Qt shl* represent the fixed heat load and the transferable heat load respectively, the transferable heat load can be shifted in a certain proportion according to the user's comfort and energy adequacy; *Qmax shl* represents the upper limit of the transferable heat load.

In order to ensure the safe and reliable operation of the integrated energy system, it is necessary to consider system constraints, including power balance constraints and unit output constraints, as well as unit creep constraints, in the context of a clear objective function [20].

1) Supply balance constraints

Power must be balanced throughout the transmission of electricity in the network, and this balance characteristic has a decisive influence on the frequency stability and voltage stability of the network. If the power generated is greater than the required load, the grid frequency will then increase

Тип лицензии CC: Attribution 4.0 International (CC BY 4.0)

Т. 8. №8. 2022
https://doi.org/10.33619/2414-2948/81

and conversely decrease, and the stability of the power system should depend on the stability of the network frequency.

$$P_{WT}^{t} + P_{PV}^{t} + P_{GT}^{t} + P_{bt.dis}^{t} = P_{fel}^{t} + P_{sel}^{t} + P_{bt.chr}^{t} \quad (27)$$

where *Pt WT* and *Pt PV* denote the output electric power of wind turbine and photovoltaic unit respectively.

2) Heat balance constraints

In a heat supply system, a balance must be maintained between the supply and demand of consumers and heat sources. The temperature of the heat supply rises as the demand of the heat consumers decreases and vice versa, and the quality of the heat supply depends to some extent on the temperature of the heat supply, thus ensuring that there is a need to dispatch results in line with the demand for heat. In this paper, heat losses due to transmission are not considered and the heat supply balance is constrained as follows:

$$H_{WHB}^{t} + H_{GB}^{t} + H_{tst.dis}^{t} = H_{fhl}^{t} + H_{shl}^{t} + H_{tst.ch}^{t} \quad (28)$$

3) Exchange power constraints

$$P_{grid.\min} \le P_{grid}^{t} \le P_{grid.\max} \quad (29)$$

$$P_{grid.down} \le P_{grid}^{t} - P_{grid}^{t-1} \le P_{grid.up} \quad (30)$$

Where: $P_{grid.max}/P_{grid.min}$ and $P_{grid.up}/P_{grid.down}$ are the maximum/small, purchased power and the upper/lower climbing rate limits of the grid respectively.

For the above master-slave game model, this paper uses a distributed optimization algorithm to optimize the solution of the return function of each investment body. The decision of the leader integrated energy operator is a class of large-scale nonlinear programming, which can be solved using a differential evolutionary algorithm to reduce the difficulty of solving, and the optimization objective of the follower user can be modeled by Yalmip and call Cplex solving tool to speed up the algorithm and ensure the accuracy of the result.

The upper-level optimization algorithm includes the following steps:

Step 1: Input initial data and set parameters, including the typical daily electric, thermal and cooling load power of the customer, the predicted wind turbine and PV output, the operating parameters of each device and the upper and lower bound constraints on the multi-energy price.

Step 2: Initialise the population *a* such that the number of iterations $K = 0$.

Step 3: The integrated energy operator sends the optimised sold energy price down to the lower-level user follower.

Step 4: The user invokes the lower layer algorithm to calculate its own revenue.

Step 5: The integrated energy operator calculates its own objective function U_1 based on equation 12.

Step 6: Crossover and mutation operations are performed on population *a* to obtain a new population *b*.

Тип лицензии CC: Attribution 4.0 International (CC BY 4.0)

Т. 8. №8. 2022
https://doi.org/10.33619/2414-2948/81

Step 7: The lower layer algorithm is invoked again to solve the follower objective function in an optimisation search and the optimisation result is sent to the upper layer integrated energy operator, which calculates its own objective function U_2 according to equation 12.

Step 8: Select the operation, if $U2>U1$, then $a=b$ and $U1=U2$, if $U2<U1$, then keep the same.

Step 9: Determine if the number of iterations is satisfied, if so, output the optimal result, otherwise skip to step 6.

The lower-level algorithm consists of the following steps:

Step 1: The user invokes the Cplex solver tool to calculate the user's electrical, thermal and cooling adjustable loads according to equation 19.

Step 2: Optimisation results are sent to the upper level leader.

This paper is based on a combined cooling, heating and power RIES, which considers multiple forms of energy, including new and renewable energy sources, to achieve a self-sustaining recycling system. The electricity and heat demand loads of the users, PV and wind turbine forecast output plans are shown in Figure 2.

Let the customer's transferable electrical load be 20% of the total demand electrical load and the adjustable thermal load be 10% of the demand thermal load due to the high sensitivity of the customer to thermal discomfort and the difficulty of regulation. The constant coefficients of user preference for electricity and heat/cooling energy are $v_e, u_e, v_{h/c}$ and $u_{h/c}$ are 1.8, 0.0012, 1.4, 0.001 respectively. the fuel cost coefficients a_e, b_e and c_e ($a_{h/c}, b_{h/c}$ and $c_{h/c}$) of the integrated energy operator are 0.0015, 0.16, 0 (0.0008, 0.13, 0) respectively, and other equipment parameters as shown in Table 1. The energy storage equipment parameters are shown in Tab 2. The RIES economic parameters are shown in Table 3.

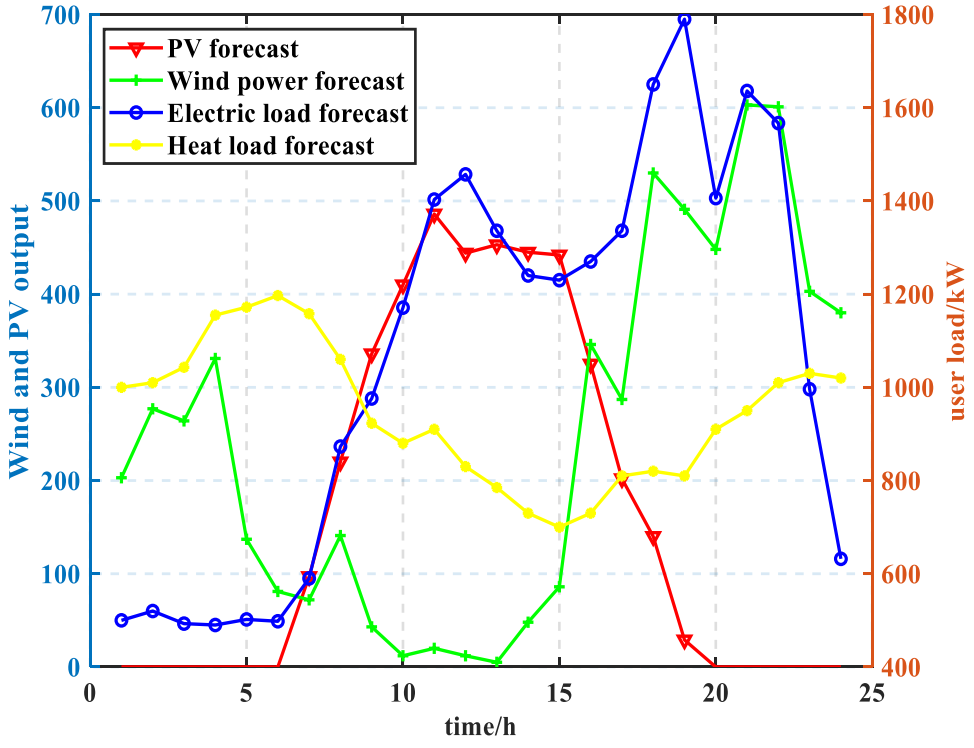

Figure 2. Forecast curves for wind, PV and customer loads

Тип лицензии CC: Attribution 4.0 International (CC BY 4.0)

Т. 8. №8. 2022
https://doi.org/10.33619/2414-2948/81

Table 1

NEW ENERGY CCHP SYSTEM PARAMETERS

Parameters	*Value*
Gas generator capacity/kW	500
Gas boiler capacity/kW	800
Electrical efficiency of generators	0.35
Waste heat recovery efficiency	0.83
Heat exchanger efficiency	0.80

Table 2

ENERGY STORAGE DEVICE EQUIPMENT PARAMETERS

Parameters	*Value*
Pmin bt.chr，*Pmax bt.chr*	0，350
Pmin bt.dis，*Pmax bt.dis*	0，350
Hmin tst.chr，*Hmax tst chr*	0，350
Hmin tst.dis，*Hmax tst dis*	0，300
ηtst.chr，*ηtst.dis*	0.98，0.98
ηbt.chr，*ηbt.dis*	0.97，0.97

Table 3

RIES ECONOMIC PARAMETERS

Parameters		*Value/ ¥/kWh*
Time share tariff	Peak	1.25
	Flat value	0.80
	Valley value	0.40
Feed-in Tariff		0.35
Heat Price Cap		0.50
Lower limit of thermal price		0.20

Table 4

RIES ECONOMIC PARAMETERS

Average electricity sales price	0.75
Average hot price	0.45

Analysis of simulation results

From the simulation results, the iterative convergence results of the integrated energy operator and the user are shown in Figure 3, convergence is reached at around 185 iterations. In the lower level game, users adjust their own energy consumption strategy in conjunction with the upper level leader's energy price, and their revenue function fluctuates. The above game analysis gives a good picture of the game process between the two parties. Once the Nash equilibrium of the game is reached, their strategies do not change anymore, and finally, the leader integrated energy operator has a gain of 4470.95¥ and follows the customer consumer surplus of 17752.8¥.

Тип лицензии CC: Attribution 4.0 International (CC BY 4.0)

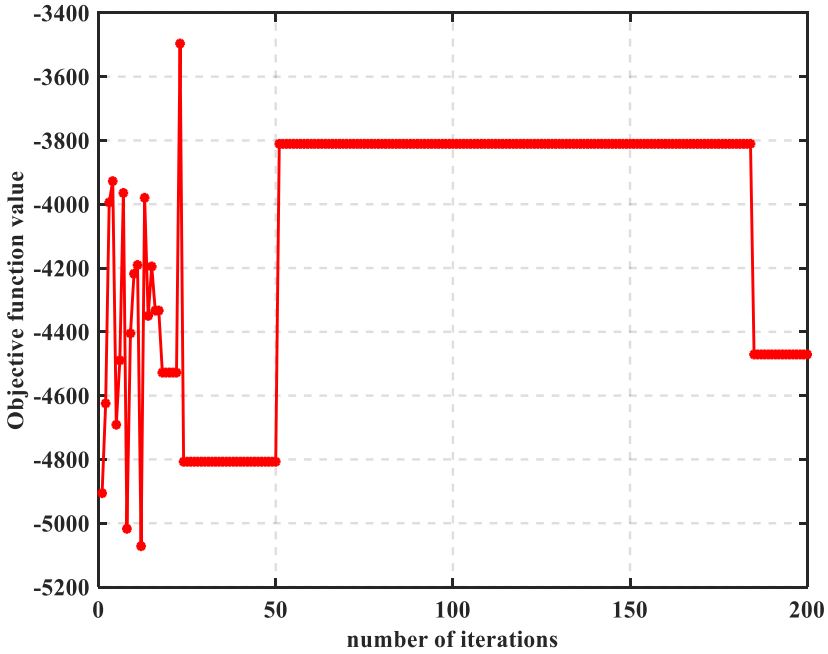

(a) DE upper level objective function curve

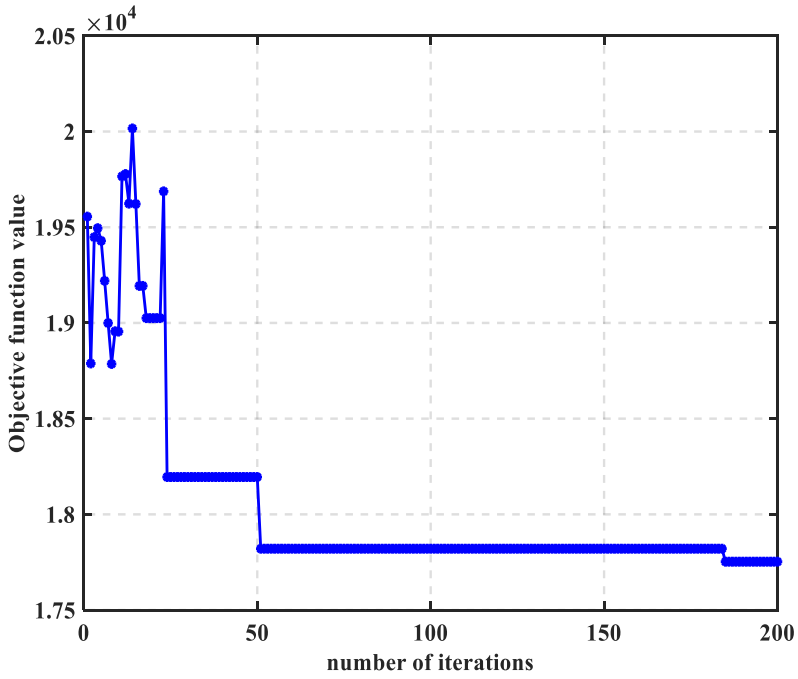

(b) DE lower level objective function curve

Figure 3. Stackelberg equilibrium convergence results

The pricing strategy of the upper tier leader operator is shown in Figure 3. The red dashed line and the green dashed line are the time-of-use tariff and feed-in tariff respectively when interacting with the larger grid. The operator's tariff strategy is always contained between the larger grid pricing to prioritise the consumption of new energy in the system, providing a better price for the energy end. From Figure 4 (a), the fluctuating trend of the operator's electricity sales price is in line with the big grid time-of-use tariff, with the aim of incentivising customers to actively purchase electricity, and

Тип лицензии CC: Attribution 4.0 International (CC BY 4.0)

Т. 8. №8. 2022
https://doi.org/10.33619/2414-2948/81

similarly, the analysis of the heat price is like the electricity price. From Figure 4 (b), there is a link between its heat purchase price and the trend of customers' heat load.

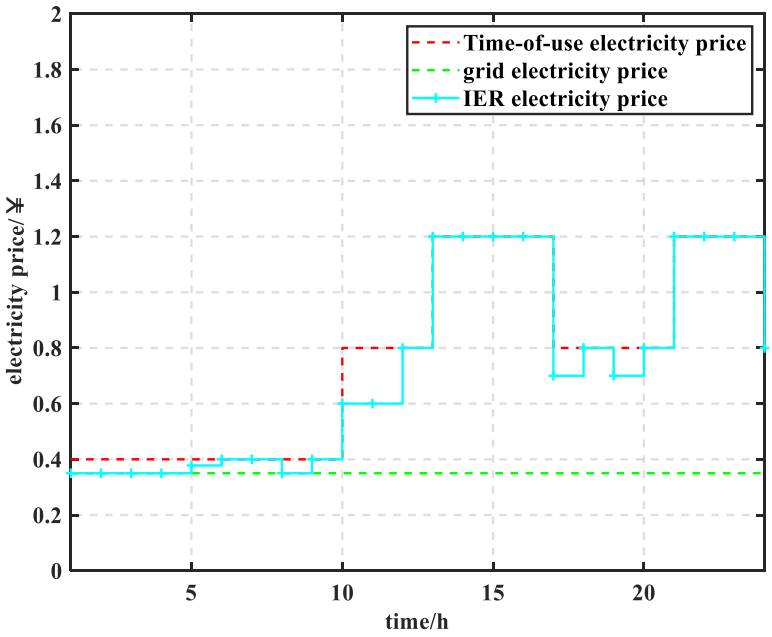

(a) Tariff results

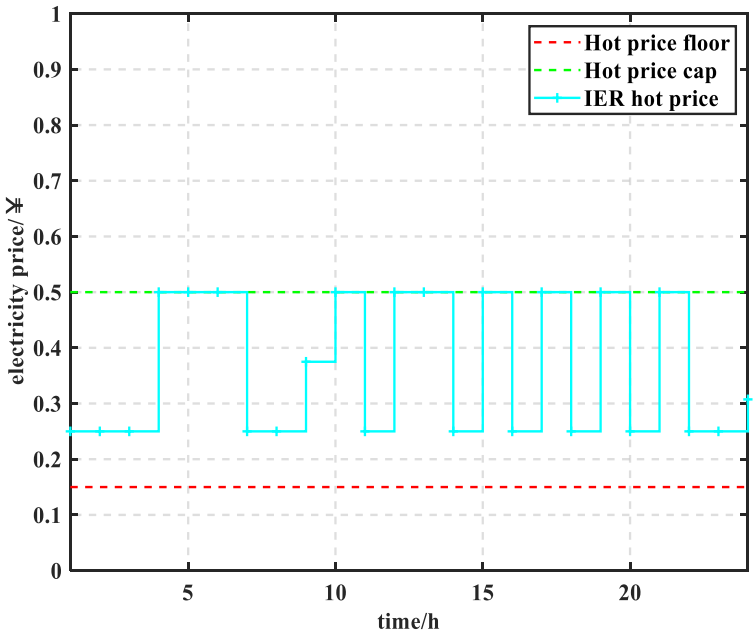

(b) Hot Price Results

Figure 4. Integrated Energy Operations Pricing Strategy

The electric and thermal load curves before and after demand response on the customer side are shown in Figure 5. From Figure 5(a), it can be seen that the load curves before and after demand response exhibit a "peak-shaving" characteristic in order to reduce the total cost of electricity under the tariff incentive. The two peaks in the consumer's original load curve occur at 11:00-12:00 and

Тип лицензии CC: Attribution 4.0 International (CC BY 4.0)

Т. 8. №8. 2022
https://doi.org/10.33619/2414-2948/81

18:00-22:00, when the tariff is higher, and after customer-side optimisation, the peak load drops significantly, shifting to 0:00-8:00 and 23:00 -24:00 when the tariff is lower in the load valley phase, the fluctuation of the electrical load curve is significantly reduced. As can be seen from Figure 5(b), the customer thermal load follows roughly the same trend as the electrical load, and the amount of thermal load shifted is relatively small in order to ensure the comfort of the customer.

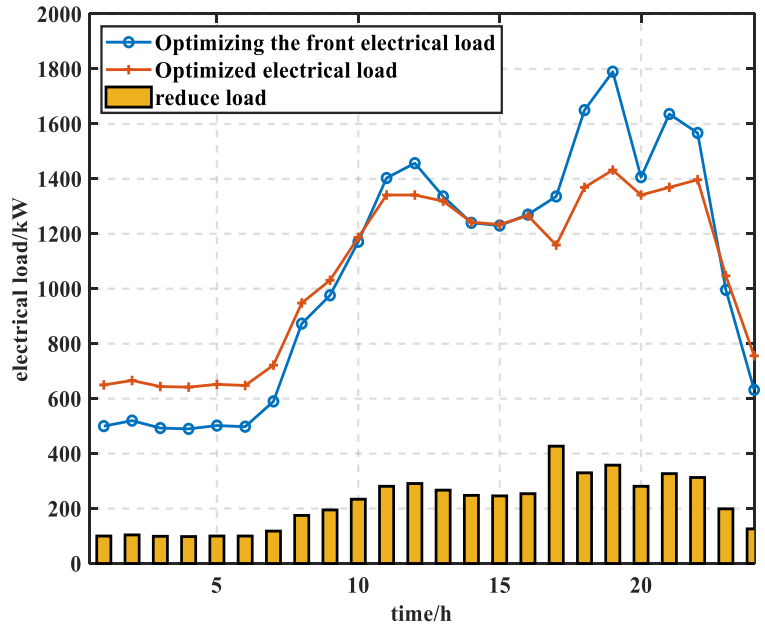

(a) Electric load curve before and after demand response

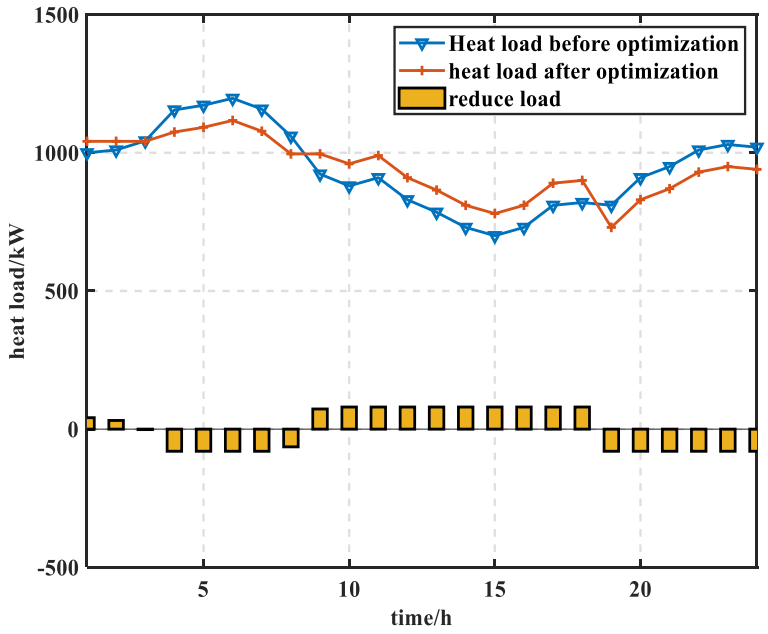

(b) Heat load curve before and after demand response

Figure 5. User load optimization curves before and after demand response

In this paper, we assume that the fuel cost of clean energy such as photovoltaic and wind turbine is approximately 0, and considering the environmental protection of new energy, the integrated energy operator gives priority to the consumption of new energy generation. From the dispatch results of

Тип лицензии CC: Attribution 4.0 International (CC BY 4.0)

Т. 8. №8. 2022
https://doi.org/10.33619/2414-2948/81

Figure 6 and Figure 7 for electric and thermal energy, we can see that during the valley hours of 23:00-7:00 for electricity consumption, the electricity consumption of customers is low, when the electricity price is in the valley, and the electric load is mainly provided by the electric load is mainly provided by the wind turbine output, and the shortage is supplemented by the gas turbine. In order to ensure heat supply, the operator directs the boiler output through price response and the heat load is mainly provided by the waste heat boiler and the gas boiler, with the shortfall being supplemented by the ESO's storage tank through low charge and high discharge. During the normal period of electricity consumption, the demand for electricity rises gradually, the wind and photovoltaic output is fully absorbed and the gas turbine output increases, with the shortfall being compensated by interaction with the main grid. The heat load is still provided by waste heat boilers and gas boilers, with the shortfall being supplemented by thermal storage tanks. The analysis during peak electricity consumption periods is similar and will not be repeated here.

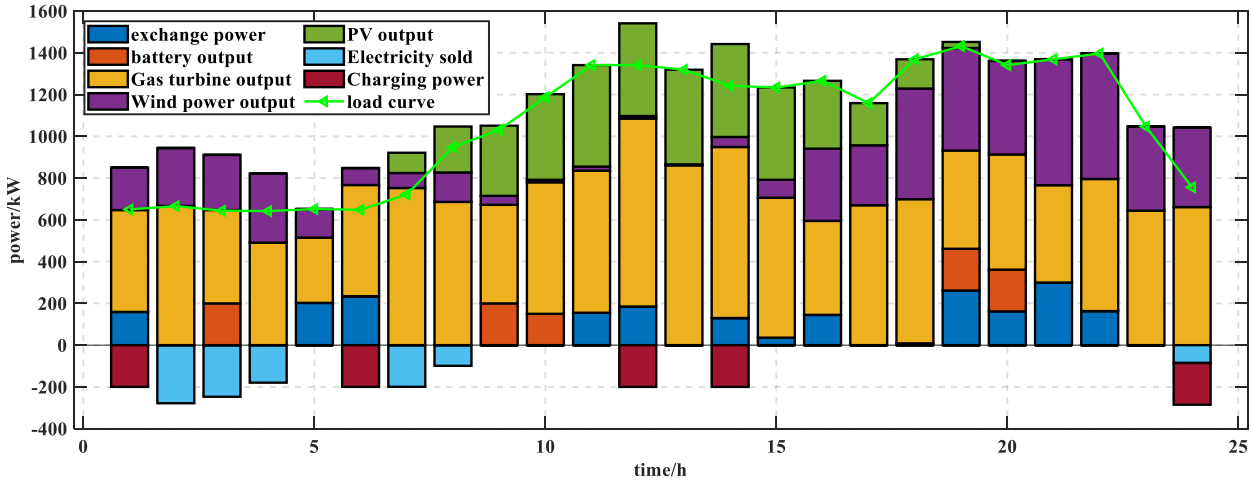

Figure 6. Electricity balance dispatch results

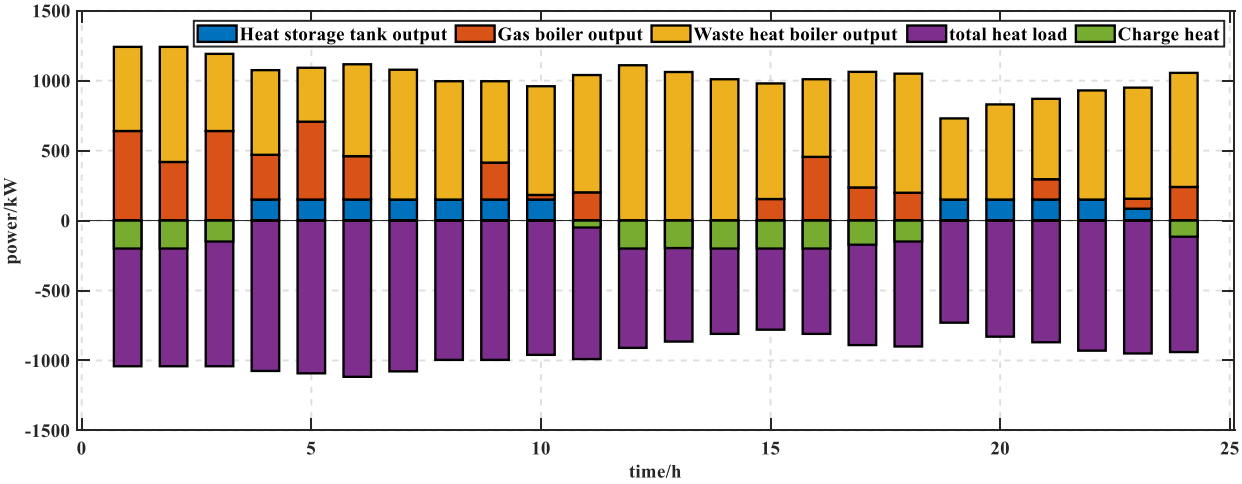

Figure 7. Heat balance scheduling results

Conclusion

In this paper, we study the dynamic pricing and energy management of an integrated electric and thermal energy system through the Stackelberg game approach. For the upper-level leader problem, we take the overall revenue of the integrated energy system as the objective function and consider constraints such as the price of electricity and the price of heat. The Stackelberg game model

Тип лицензии CC: Attribution 4.0 International (CC BY 4.0)

is constructed with the highest customer satisfaction as the objective function, and the power balance and heat balance of the system are also considered. The simulation results show that the proposed model not only effectively weighs the interests of the integrated energy system and the customer aggregator, but also achieves a win-win situation for both the customer aggregator and the external grid, and the solution algorithm used protects the data privacy between the integrated energy system and the customer aggregator.

References:

1. Li, H., Liu, D., & Yao, D. Y. (2021). Analysis and reflection on the development of power system towards the goal of carbon emission peak and carbon neutrality. *Proc. CSEE*, *41*, 6245-6259.

2. Li, X., Ai, X., Hu, J., Zhou, B., & Lin, Z. (2019). Three-stage combined peak regulation strategy for nuclear-thermal-virtual power plant considering carbon trading mechanism. *Power Syst. Technol*, *43*, 2460-2470.

3. Wu, C., Lin, S., Xia, C., & Guan, L. (2020). Distributed optimal dispatch of microgrid cluster based on model predictive control. *Power Syst. Technol.*, *44*(2), 530-538.

4. Khan, M. R. B., Jidin, R., & Pasupuleti, J. (2016). Multi-agent based distributed control architecture for microgrid energy management and optimization. *Energy Conversion and Management*, *112*, 288-307. https://doi.org/10.1016/j.enconman.2016.01.011

5. Dou, C., Jia, X., & Heng, L. I. (2016). Multi-agent-system-based market bidding strategy for distributed generation in microgrid. *Power System Technology*, *40*(2), 579-586.

6. Lee, J., Guo, J., Choi, J. K., & Zukerman, M. (2015). Distributed energy trading in microgrids: A game-theoretic model and its equilibrium analysis. *IEEE Transactions on Industrial Electronics*, *62*(6), 3524-3533. https://doi.org/10.1109/TIE.2014.2387340

7. Jadhav, A. M., & Patne, N. R. (2017). Priority-based energy scheduling in a smart distributed network with multiple microgrids. *IEEE Transactions on Industrial Informatics*, *13*(6), 3134-3143. https://doi.org/10.1109/TII.2017.2671923

8. Jadhav, A. M., Patne, N. R., & Guerrero, J. M. (2018). A novel approach to neighborhood fair energy trading in a distribution network of multiple microgrid clusters. *IEEE Transactions on Industrial Electronics*, *66*(2), 1520-1531. https://doi.org/10.1109/TIE.2018.2815945

9. Zhong, W., Xie, S., Xie, K., Yang, Q., & Xie, L. (2020). Cooperative P2P energy trading in active distribution networks: An MILP-based Nash bargaining solution. *IEEE Transactions on Smart Grid*, *12*(2), 1264-1276. https://doi.org/10.1109/TSG.2020.3031013

10. Sheng, W., Wu, M., Ji, Y., Kou, L., Pan, J., Shi, H., ... & Wang, Z. G. (2019, April). Key techniques and engineering practice of distributed renewable generation clusters integration. In *Proceedings of the CSEE* (Vol. 39, No. 8, pp. 2175–2186).

11. Mu, C., Ding, T., Dong, J., Ning, K., Dong, X., & He, Y. (2021). Development of decentralized peer-to-peer multi-energy trading system based on private blockchain technology. *Journal of Proceedings of the CSEE*.

12. Doan, H. T., Cho, J., & Kim, D. (2021). Peer-to-peer energy trading in smart grid through blockchain: A double auction-based game theoretic approach. *Ieee Access*, *9*, 49206–49218. https://doi.org/10.1109/ACCESS.2021.3068730

13. Yang, Z., Peng, S., Liao, Q., Liu, D., Xu, Y., & Zhang, Y. J. (2018). Non-cooperative trading method for three market entities in integrated community energy system. *Autom. Electr. Power Syst*, *42*(14), 32-39.

14. Park, S., Lee, J., Bae, S., Hwang, G., & Choi, J. K. (2016). Contribution-based energy-trading mechanism in microgrids for future smart grid: A game theoretic approach. *IEEE Transactions on Industrial Electronics*, *63*(7), 4255-4265. https://doi.org/10.1109/TIE.2016.2532842

Тип лицензии CC: Attribution 4.0 International (CC BY 4.0)

15. Liu, N., Cheng, M., Yu, X., Zhong, J., & Lei, J. (2018). Energy-sharing provider for PV prosumer clusters: A hybrid approach using stochastic programming and stackelberg game. *IEEE Transactions on Industrial Electronics*, *65*(8), 6740-6750. https://doi.org/10.1109/TIE.2018.2793181

16. Cui, S., Wang, Y. W., Shi, Y., & Xiao, J. W. (2020). Community energy cooperation with the presence of cheating behaviors. *IEEE Transactions on Smart Grid*, *12*(1), 561-573. https://doi.org/10.1109/TSG.2020.3022792

17. Mei, Shengwei, Liu, Feng, Wei, Wei. (2016). Fundamentals of engineering game theory and power system application. Beijing Science Press.

18. Paudel, A., Chaudhari, K., Long, C., & Gooi, H. B. (2018). Peer-to-peer energy trading in a prosumer-based community microgrid: A game-theoretic model. *IEEE Transactions on Industrial electronics*, *66*(8), 6087-6097. https://doi.org/10.1109/TIE.2018.2874578

19. Liu, N., Yu, X., Wang, C., Li, C., Ma, L., & Lei, J. (2017). Energy-sharing model with price-based demand response for microgrids of peer-to-peer prosumers. *IEEE Transactions on Power Systems*, *32*(5), 3569-3583. https://doi.org/10.1109/TPWRS.2017.2649558

20. Xu, Y., Liao, Q., Liu, D., Peng, S., Yang, Z., Zou, H., & Zhang, L. (2019). Multi-player intraday optimal dispatch of integrated energy system based on integrated demand response and games. *Power System Technology*, *43*(7), 2506-2518.

Список литературы:

1. Li H., Liu D., Yao D. Y. Analysis and reflection on the development of power system towards the goal of carbon emission peak and carbon neutrality // Proc. CSEE. 2021. V. 41. P. 6245-6259.

2. Li X., Ai X., Hu J., Zhou B., Lin, Z. Three-stage combined peak regulation strategy for nuclear-thermal-virtual power plant considering carbon trading mechanism // Power Syst. Technol. 2019. V. 43. P. 2460-2470.

3. Wu C., Lin S., Xia C., Guan L. Distributed optimal dispatch of microgrid cluster based on model predictive control // Power Syst. Technol. 2020. V. 44. №2. P. 530-538.

4. Khan M. R. B., Jidin R., Pasupuleti J. Multi-agent based distributed control architecture for microgrid energy management and optimization // Energy Conversion and Management. 2016. V. 112. P. 288-307. https://doi.org/10.1016/j.enconman.2016.01.011

5. Dou C., Jia X., Heng L. I. Multi-agent-system-based market bidding strategy for distributed generation in microgrid // Power System Technology. 2016. V. 40. №2. P. 579-586.

6. Lee J., Guo J., Choi J. K., Zukerman M. Distributed energy trading in microgrids: A game-theoretic model and its equilibrium analysis // IEEE Transactions on Industrial Electronics. 2015. V. 62. №6. P. 3524-3533. https://doi.org/10.1109/TIE.2014.2387340

7. Jadhav A. M., Patne N. R. Priority-based energy scheduling in a smart distributed network with multiple microgrids //IEEE Transactions on Industrial Informatics. – 2017. – Т. 13. – №. 6. – С. 3134-3143. https://doi.org/10.1109/TII.2017.2671923

8. Jadhav A. M., Patne N. R., Guerrero J. M. A novel approach to neighborhood fair energy trading in a distribution network of multiple microgrid clusters // IEEE Transactions on Industrial Electronics. 2018. V. 66. №2. P. 1520-1531. https://doi.org/10.1109/TIE.2018.2815945

9. Zhong W., Xie S., Xie K., Yang Q., Xie L. Cooperative P2P energy trading in active distribution networks: An MILP-based Nash bargaining solution // IEEE Transactions on Smart Grid. 2020. V. 12. №2. P. 1264-1276. https://doi.org/10.1109/TSG.2020.3031013

10. Sheng W., Wu M., Ji Y., Kou L., Pan J., Shi H., Wang Z. G. Key techniques and engineering practice of distributed renewable generation clusters integration // Proceedings of the CSEE. 2019. V. 39. №8. P. 2175-2186.

Тип лицензии CC: Attribution 4.0 International (CC BY 4.0)

11. Mu C., Ding T., Dong J., Ning K., Dong X., He Y. Development of decentralized peer-to-peer multi-energy trading system based on private blockchain technology // Journal of Proceedings of the CSEE. 2021.

12. Doan H. T., Cho J., Kim D. Peer-to-peer energy trading in smart grid through blockchain: A double auction-based game theoretic approach // Ieee Access. 2021. V. 9. P. 49206-49218. https://doi.org/10.1109/ACCESS.2021.3068730

13. Yang Z., Peng S., Liao Q., Liu D., Xu Y., Zhang Y. J. Non-cooperative trading method for three market entities in integrated community energy system // Autom. Electr. Power Syst. 2018. V. 42. №14. P. 32-39.

14. Park S., Lee J., Bae S., Hwang G., Choi J. K. Contribution-based energy-trading mechanism in microgrids for future smart grid: A game theoretic approach // IEEE Transactions on Industrial Electronics. 2016. V. 63. №7. P. 4255-4265. https://doi.org/10.1109/TIE.2016.2532842

15. Liu N., Cheng M., Yu X., Zhong J., Lei J. Energy-sharing provider for PV prosumer clusters: A hybrid approach using stochastic programming and stackelberg game // IEEE Transactions on Industrial Electronics. 2018. V. 65. №8. P. 6740-6750. https://doi.org/10.1109/TIE.2018.2793181

16. Cui S., Wang Y. W., Shi Y., Xiao J. W. Community energy cooperation with the presence of cheating behaviors // IEEE Transactions on Smart Grid. 2020. V. 12. №1. P. 561-573. https://doi.org/10.1109/TSG.2020.3022792

17. Mei Shengwei, Liu Feng, Wei Wei. Fundamentals of engineering game theory and power system application. Beijing Science Press, 2016.

18. Paudel A., Chaudhari K., Long C., Gooi H. B. Peer-to-peer energy trading in a prosumer-based community microgrid: A game-theoretic model // IEEE Transactions on Industrial electronics. 2018. V. 66. №8. P. 6087-6097. https://doi.org/10.1109/TIE.2018.2874578

19. Liu N., Yu X., Wang C., Li C., Ma L., Lei J. Energy-sharing model with price-based demand response for microgrids of peer-to-peer prosumers // IEEE Transactions on Power Systems. 2017. V. 32. №5. P. 3569-3583. https://doi.org/10.1109/TPWRS.2017.2649558

20. Xu Y., Liao Q., Liu D., Peng S., Yang Z., Zou H., Zhang L. Multi-player intraday optimal dispatch of integrated energy system based on integrated demand response and games // Power System Technology. 2019. V. 43. №7. P. 2506-2518.

Работа поступила
в редакцию 08.07.2022 г.

Принята к публикации
12.07.2022 г.

Ссылка для цитирования:

Wang Yibo, Feng Guozeng Dynamic Pricing and Energy Management of Electric Heating Integrated Energy System Based on Stackelberg Game // Бюллетень науки и практики. 2022. Т. 8. №8. С. 245-262. https://doi.org/10.33619/2414-2948/81/28

Cite as (APA):

Wang, Yibo, & Feng, Guozeng, (2022). Dynamic Pricing and Energy Management of Electric Heating Integrated Energy System Based on Stackelberg Game. *Bulletin of Science and Practice, 8*(8), 245-262. https://doi.org/10.33619/2414-2948/81/28

Тип лицензии CC: Attribution 4.0 International (CC BY 4.0)